Chemical Physics 124 (1988) 265–272
North-Holland, Amsterdam

MECHANISM OF THE REACTION $NH(^1\Delta)+NO \rightarrow N_2O+H$ IN THE GAS PHASE

Takayuki FUENO, Masayuki FUKUDA and Keiichi YOKOYAMA
Department of Chemistry, Faculty of Engineering Science, Osaka University, Toyonaka, Osaka 560, Japan

Received 5 October 1987; in final form 29 April 1988

Hydrazoic acid HN_3 was photolyzed in the presence of a controlled amount of NO in the gas phase, to investigate the reaction of $NH(^1\Delta)$ with NO. Ab initio CI studies indicate that the ultimate product should be N_2O, which would arise via an intermediacy of the adduct radical $HNNO(^2A')$. Mass-spectrometric analyses of the reaction mixtures have shown that N_2O is indeed a principal product but that a sizable quantity of H_2O has been formed concurrently. Quantum yields of N_2O are found to increase in proportion to the initial molar fractions of NO in the reactant gas mixtures used. It is concluded that $NH(^1\Delta)$ enters into capture (no-barrier) reactions with NO and HN_3 in a competitive manner, to give N_2O and NH_2, respectively, the latter product eventually leading to H_2O through a rapid capture reaction with excess NO.

1. Introduction

The imino radical in its lowest singlet state, $NH(a\,^1\Delta)$, can insert into a single bond of paraffins to give amines and, at the same time, directly abstracts a hydrogen atom giving rise to the amino radical [1]:

$$NH(^1\Delta)+H\text{–}R \longrightarrow H_2NR\,, \qquad (1a)$$
$$\longrightarrow NH_2+R\,. \qquad (1b)$$

Obviously, reaction (1a) is a concerted process with virtually no activation energy, whereas reaction (1b) is an activation-controlled process. The activation barrier heights for reaction (1b) are, however, generally so low as to permit the hydrogen abstraction to compete with the insertion (1a), as has been demonstrated theoretically [2]. More important in this context is the notion that this dual chemical behavior of $NH(^1\Delta)$ is a consequence of the duality in its electronic structure. Thus, the insertion capability is ascribable to the closed-shell-like character of the $^1\Delta$ state which can be represented by the two-configurational (x^2-y^2) wavefunction, while the abstraction mode is due to the diradical property arising from its open-shell (xy) character [3–5].

Inasmuch as $NH(^1\Delta)$ in its open-shell form can be regarded as a singlet diradical, its diradical character ought to be revealed most eminently when it is allowed to react with radical species. Thus, the association reactions of $NH(^1\Delta)$ with doublet radicals are thought to constitute another important type of elementary reactions possible to $NH(^1\Delta)$.

Motivated by the above-delineated perspective, we have undertaken to investigate the reaction of $NH(^1\Delta)$ with NO as a doublet radical. Ab initio SCF computations followed by the configuration-interaction (CI) treatments indicate that the association product HN–NO is liable to be collapsed into N_2O and H:

$$NH(^1\Delta)+NO \rightarrow [NH\text{–}NO] \rightarrow N_2O+H\,. \qquad (2)$$

The possibility of a similar type of reaction for the case of $NH(^3\Sigma^-)$ has been suggested by Melius and Binkley [6].

The purpose of the present work is to clarify the dynamical mechanism of reaction (2) theoretically and to confirm the formation of nitrous oxide N_2O experimentally. To this end, the path as well as the energetics of reaction (2) have been examined theoretically, and the quantum yields of N_2O under varying conditions have been determined experimentally. Rather unexpectedly, it has been observed that a sizable amount of H_2O is formed concurrently with N_2O. The overall mechanism of reactions will be discussed

in the light of the theoretical as well as the experimental results obtained.

2. Methods

2.1. Theoretical calculations

The potential energy profiles for the reactions of both $NH(X\,^3\Sigma^-)$ and $NH(a\,^1\Delta)$ with NO have been examined by ab initio MO calculations. The basis sets used are the conventional split-valence 4-31G functions [7] augmented with one set each of polarization functions for every atom involved. The exponents used for the polarization functions are $\zeta_p(H)=1.1$ and $\zeta_d(N)=\zeta_d(O)=0.8$ [8].

The minimum-energy paths for reactions were traced by the UHF SCF procedure, using the GAUSSIAN 80 program package [9]. Geometries for the stable energy minima and the energy saddle points (transition states, TS) were all SCF-optimized. The transition state geometries were all checked with the vibrational normal-mode analyses.

All the transition states located as well as the relevant energy-minimum structures were subjected to the multireference double-excitation (MRD) configuration-interaction (CI) computations (4-31G**//4-31G**). The TABLE MRD CI program furnished by Buenker [10,11] was used. The configurations whose contributions $|c_i|^2$ to a state exceed 0.5% were all regarded as the main (reference) configurations. The lowest configuration-selection threshold T was deliberately assigned a value between 1 and 10 μhartree, so that the maximal dimension of the configurational space fell in the region 7000–9000. Four successive threshold values increasing stepwise by 5 μhartree each were used to obtain the CI energy $E_{CI,T\rightarrow 0}$ extrapolated to $T=0$ hartree. The generalized Langhoff–Davidson approximation [12,13] was used to correct for possible errors which might arise from the use of a limited number of reference configurations. The CI energies thus corrected are regarded as estimates of full CI values [13,14] and will be denoted as E_{CI}.

2.2. Experimental

Mixtures of 1–7 Torr of HN_3 with 3–40 Torr of NO and 0–200 Torr of SF_6 were photolyzed for 0.5–4 h at room temperature. The light source used was a 450 W medium-pressure mercury lamp (Ushio UM-452). A combination of solution filters (aq. $NiSO_4$, aq. $CoSO_4$ and a cyclohexane solution of 1,4-diphenyl-1,3-butadiene) was used to isolate the 254 nm light for the photolysis. The effective band pass of the combined filters was 240–270 nm. The photolyzing light collimated by a quartz lens ($f=110$ mm) was led into a reaction cell. The reaction cell used was a quartz cylinder of 102 mm in length and 12 mm in diameter. The light that had passed through the cell was collected in a phototube (Hamamatsu Photonics R-840) for recording.

After the photolysis, the reaction mixture was kept at −196°C for ≈1 h. The condensate was degassed at −196°C and, after having been allowed to stand at room temperature for ≈1 h, was subjected to gas-chromatographic analysis. A 2.5 m column of Porapak Q was used at 25°C with a stream (18 cm^3/min) of He as carrier. The principal product was identified to be N_2O; the observed retention time 4.5 min agreed with that for an authentic gas sample of N_2O.

Determinations of N_2O formed were conducted on a quadrupole mass spectrometer (ULVAC MSQ-150A). In preliminary experiments, it was found that the mass signal for SF^+ ($m/e=51$) as a fragment ion from SF_6 was stable enough to be used as a reference for the determination of N_2O. The relative peak heights for N_2O^+ ($m/e=44$) and SF^+ were calibrated for gas mixtures of N_2O and SF_6 of known concentrations. It was confirmed that the peak-height ratios stayed invariant during the time interval (usually 10 min) required for the analysis. The nonvolatiles (at −196°C) of the reaction gas mixtures were introduced into the ionization room of the mass spectrometer through a variable-leak bulb at room temperature. The mass spectra were recorded on a penrecorder.

The $NH(^1\Delta)$ radicals generated by the present photolysis are typically ≈1% of the HN_3 sample used. The total amount of NH generated in each run can be assumed to equal the total number of photons absorbed in the photolysis, since the quantum yield of $NH(^1\Delta)$ from HN_3 by the 254 nm light is known to be nearly 1.0 [15]. The amount of photons absorbed was calculated from the amount of the incident photons, using the absorption coefficient of HN_3 previ-

ously determined (254 nm at 23°C), 1.40×10^{-3} $Torr^{-1}$ cm^{-1} [1]. The intensity of the incident light was measured with a phototube calibrated by chemical actinometry. A $K_3Fe(C_2O_4)_3$–1,10-phenanthrolin system was used for the chemical actinometry [16].

The quantum yields of N_2O were obtained from the total amount of N_2O formed and the amount of photons absorbed by the reaction mixture. The N_2O quantum yields are thus the molar yields of N_2O formed per one mole of $NH(^1\Delta)$ generated.

HN_3 was synthesized and purified by the method described elsewhere [1]. It was stored in 5 ℓ pyrex bulb. A portion of it was degassed each time immediately prior to use. Both NO and SF_6 of high purity were purchased and used after appropriate degassing.

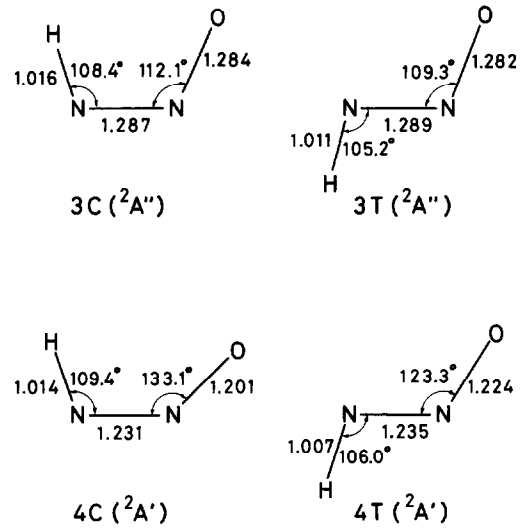

Fig. 1. Optimal geometries of the HNNO doublet radical.

3. Results

3.1. Potential energy profiles

It is presumed intuitively that the primary step of the reaction between NH and NO is the association reaction giving a doublet adduct HN–NO. Under this presumption, the optimal structure for the adduct radical was explored by the UHF SCF procedure. Two planar doublet structures are conceivable. One is a doublet ($^2A''$) of the allyl radical type with three π electrons delocalized over the NNO skeleton, while the other is such a doublet ($^2A'$) that four electrons are accommodated in the π orbitals, leaving the unpaired electron in an a′ orbital of the skeleton:

$$^2A'',\quad ...(1a'')^2(9a')^2(2a'')(10a')^2,$$

$$^2A',\quad ...(1a'')^2(9a')^2(2a'')^2(10a').$$

For either of the two doublets, the cis and trans forms are possible. These four structures will be denoted as 3C, 3T, 4C and 4T. Thus, 4T, for example, should be read as indicating the four-π-electron form ($^2A'$) in the trans arrangement of the four atoms. The optimized geometries for the four radicals are given in fig. 1.

Tracings of the minimum-energy paths by the SCF procedure have indicated that both 4C and 4T are connected with $NH(^1\Delta)+NO$, whereas 3C and 3T with $NH(^3\Sigma^-)+NO$. Clearly, $NH(^3\Sigma^-)$ attacks the singly occupied orbital (a′) localized on the N atom of NO. The $NH(^1\Delta)$ radical, on the other hand, appears to attack the π bond orbital of NO.

MRD CI calculations for the SCF optimized geometries have shown that the effects of electron correlation are much greater in the $^2A'$ radicals (4C and 4T) than in the $^2A''$ radicals (3C and 3T), as can be seen in table 1. In terms of the CI energy E_{CI}, the former doublets are significantly more stable than the latter, the total energies of the four radicals relative to the $NH(^3\Sigma^-)+NO$ system as a common reference being −77 (3C), 54 (3T), −252 (4C) and −254 (4T) kJ/mol. Thus, the association reaction of our present concern,

$$NH(^1\Delta)+NO \rightarrow NH\text{–}NO(^2A'), \tag{3}$$

is predicted to have an exothermicity of ≈430 kJ/mol.

Possible pathways for the subsequent fragmentation of the $^2A'$ radical are

$$HN\text{–}NO(^2A') \rightarrow HNN(^2A')+O(^3P), \tag{4a}$$

$$\rightarrow N_2O(^1\Sigma^+)+H, \tag{4b}$$

$$\rightarrow N_2+OH(^2\Pi). \tag{4c}$$

Table 1
Total energies calculated for various stationary structures

Structure		Energy (hartree)	
		SCF [a]	CI [b]
$NH(^3\Sigma^-)+NO$		−184.03215	−184.47594
$NH(^1\Delta)+NO$		−183.99897	−184.40810
$HNNO(^2A'')$	3C	−184.03300	−184.50505
	3T	−184.03429	−184.45530
$HNNO(^2A')$	4C	−184.03595	−184.57196
	4T	−184.04175	−184.57241
TS1	$4C \rightarrow N_2O+H$	−183.97633	−184.49534
TS2	$4C \rightarrow N_2+OH$	−183.97081	−184.49028
TS3	$4T \rightarrow 4C$	−183.99845	−184.52174
TS4	$HN_2 \rightarrow H+N_2$	−109.30067	−109.62258
$HN_2(^2A')$		−109.32304	−109.64895
$N_2O(^1\Sigma^+)$		−183.50573	−184.02704
$N_2(^1\Sigma_g^+)$		−108.83933	−109.15183
$NO(^2\Pi)$		−129.12300	−129.44450
$OH(^2\Pi)$		−75.31748	−75.47143

[a] UHF SCF (4-31G**) optimizations.
[b] MRD-CI (4-31G**//4-31G**) calculations.

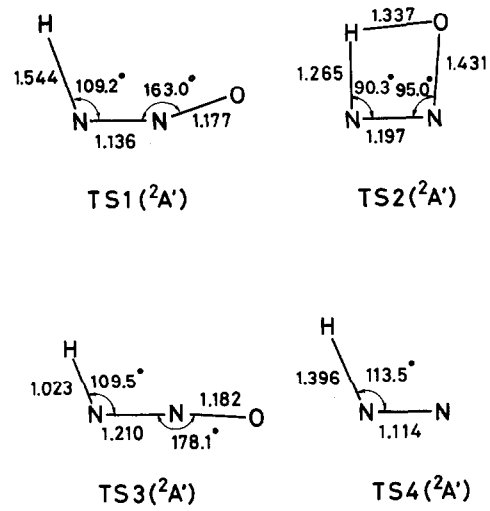

Fig. 2. Optimized transition state geometries. TS1, N–H bond leavage $4C \rightarrow N_2O+H$, reaction (4b); TS2, 1,3-hydrogen migration $4C \rightarrow N_2+OH$, reaction (4c); TS3, isomerization $4T \rightarrow 4C$; TS4, N–H bond cleavage $NH_2 \rightarrow H+N_2$.

Reaction (4a) is endothermic and has no activation barrier, whereas both reactions (4b) and (4c) should be elementary processes involving the activation energies [6]. Because reaction (4c) is possible only for the cis form of $HNNO(^2A')$, we have considered the reactions (4a)–(4c) for the 4C isomer primarily. The energy changes of reaction ΔE_{CI} calculated for reactions (4a)–(4c) are 278, 123 and −135 kJ/mol, respectively.

Geometries for the transition states, TS1 and TS2, for reactions (4b) and (4c), respectively, have been optimized by the 4-31G** SCF procedure. The optimal structures obtained are shown in fig. 2. Both geometries closely resemble those that have recently been reported by Marshall, Fontijn and Melius [17] for the same reactions.

MRD CI calculations were carried out for both TS1 and TS2 at their SCF optimized geometries. The activation barrier heights $\Delta E^{\ddagger}$ obtained for reactions (4b) and (4c) are 201 and 214 kJ/mol, respectively. It has been confirmed that use of the one-electron functions obtained by the quartet ($^4A'$) SCF calculations in place of the doublet ($^2A'$) SCF procedure does not alter the results appreciably (by no more than 5 kJ/mol). Reaction (4b) thus appears to be more favorable than reaction (4c), in agreement with the feature demonstrated by Marshall et al. [17], even though both of our $\Delta E^{\ddagger}$ values are somewhat greater than theirs. At any rate, it is clear that the adduct radical 4C formed by reaction (3) is liable to decompose spontaneously in the gas phase, inasmuch as the exothermicity for reaction (3) (430 kJ/mol) far exceeds the activation barrier heights for the subsequent fragmentation processes. The most probable path of fragmentation should be reaction (4b), which gives $N_2O(^1\Sigma^+)$.

A few words seem to be in order regarding TS1. The optimal geometry located is in a planar cis form, as is shown in fig. 2. Because TS1 is smoothly connected with 4C through the minimum-energy path over the potential energy surface, there is no doubt that 4C is subject to the N–H bond breaking reaction (4b). When the N–H bond of 4T is elongated, however, it is found that the bond angle ∠NNO increases progressively until the whole system takes on a cis structure to reach the same transition state (TS1) eventually.

In order to look into the dynamical mode of isomerization more closely, the path for the isomerization $4T \rightarrow 4C$ has been traced by the SCF procedure. As a result, it is proved that the minimum-energy path

for the isomerization is such that the O atom migrates on the molecular plane. The transition state (TS3) located is planar in geometry with the bond angle ∠NNO being nearly 180°, as is shown in fig. 2. A similar (in-plane inversion) mode of the trans–cis isomerization has been noted with diazene HN=NH [18] and difluorodiazene FN=NF [19] theoretically. For the present instance of isomerization (TS3), CI calculations have given the barrier height $\Delta E^{\ddagger}=83$ kJ/mol, which is evidently lower than the activation barrier height $\Delta E^{\ddagger}=201$ kJ/mol calculated for the N–H bond breaking reaction (4b) of 4C. No doubt, the N–H bond scission of 4T suffers the trans–cis isomerization before the scission is completed.

As for the fragmentation of the $^2A''$ radical, the energetically most favorable is the cleavage of the N–O bond:

$$HN\text{–}NO(^2A'') \rightarrow HNN(^2A') + O(^3P)\,. \qquad (5)$$

The HNN radical is liable to be decomposed into N_2+H via the transition state (TS4). The barrier height calculated by the present CI procedure is 69 kJ/mol, which does not differ greatly from the value of ≈46 kJ/mol reported by Pople et al. [20].

The overall potential energy profiles calculated for the NH+NO system are diagrammatically illustrated in fig. 3. The energy gaps given in square brackets are the empirical estimates made on the basis of the experimental thermochemical data [21]. The calculated energy gaps shown in fig. 3 will generally be accurate only to within 20 kJ/mol. Yet, they will be reliable enough to permit the conclusion that the reaction of $NH(^1\Delta)$ with NO will lead to the formation of N_2O as the principal product.

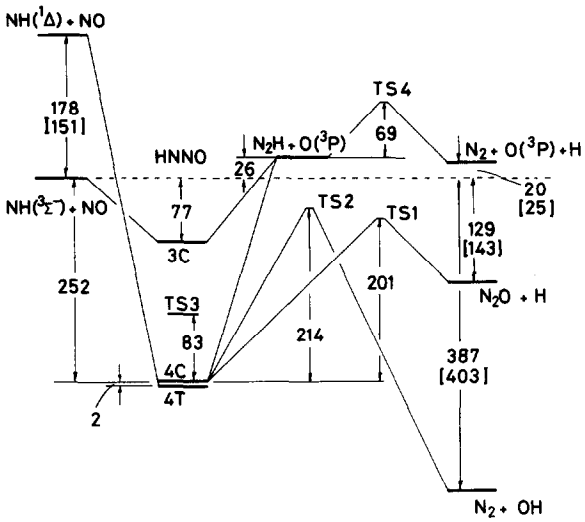

Fig. 3. Potential energy profiles calculated for the HN–NO system by the MRD-CI (4-31G**//4-31G**) procedure. The energy gaps shown are in units of kJ/mol. The values given in brackets are those obtained from the relevant thermochemical data [21].

3.2. Quantum yields of N_2O

In order to confirm that N_2O is the ultimate main product of reaction (2), we have attempted determinations of the quantum yields Φ of N_2O under various conditions. By the quantum yields we mean the yields of N_2O per one mole of $NH(^1\Delta)$ generated photochemically. Determinations of Φ entail quantitative determinations of $NH(^1\Delta)$ generated in given runs and of N_2O formed in the cell. Actinometry and mass-spectrometry have been conducted for this purpose, as has been described in section 2.2.

Table 2 gives some representative data obtained under varying initial concentrations of HN_3 and NO at room temperature. The $\Phi(N_2O)$ data listed inevitably involve experimental errors amounting to 0.05. Nevertheless, it does appear that $\Phi(N_2O)$ is increased with the increase in the initial concentration of NO, even though the reactant NO has been used always in large excess over the $NH(^1\Delta)$ radicals generated.

In fig. 4, the quantum yields $\Phi(N_2O)$ are plotted against the initial molar fraction of NO:

$$x_{NO} = [NO]_0/([HN_3]_0 + [NO]_0)\,, \qquad (6)$$

for a total of 15 runs. Although the plotted points are somewhat scattered, $\Phi(N_2O)$ does appear to be proportional, to a first approximation, to x_{NO} with the proportionality factor $\eta=0.70$. η may be understood as a partial rate factor with which the adduct radical HNNO will select the decomposition channel (4b) to give N_2O; $\eta = k_{4b}/(k_{4a}+k_{4b}+k_{4c})$.

The observed proportionality, though somewhat crude, between $\Phi(N_2O)$ and x_{NO} suggests that part of $NH(^1\Delta)$ has been consumed by reactions with the coexisting HN_3. The most probable is the hydrogen abstraction reaction as follows [22]:

Table 2
Representative data for the product determinations

No.	$[HN_3]_0$ (Torr)	$[NO]_0$ (Torr)	$[SF_6]$ (Torr)	x_{NO} [a)]	$I\Delta t$ (10^{-8} mol)	N_2O (10^{-8} mol)	H_2O (10^{-8} mol)	$\Phi(N_2O)$	$\Phi(H_2O)$
1	5.88	0.0	15.41	0.0	9.11	0.0	–	0.0	–
2	6.65	2.35	12.21	0.261	0.99	0.22		0.22	
3	4.89	3.81	10.56	0.438	3.27	0.79	1.67	0.24	0.51
4	5.16	4.10	18.58	0.443	3.28	0.86	1.43	0.25	0.44
5	3.45	3.46	20.02	0.501	2.33	0.73	0.83	0.31	0.36
6	5.59	7.17	10.99	0.562	3.25	1.37	1.40	0.36	0.43
7	5.11	12.69	111.0	0.713	1.72	0.72	0.56	0.41	0.32
8	6.21	29.69	8.32	0.827	8.12	3.42	1.96	0.42	0.24
9	1.26	29.41	11.58	0.953	1.92	1.31		0.67	

[a)] $x_{NO}=[NO]_0/([HN_3]_0+[NO]_0)$.

$$NH(^1\Delta)+HN_3\rightarrow NH_2+N_3\,. \qquad (7)$$

The quantum yield of N_2O should then be controlled by the competition between reactions (2) and (7). More precisely speaking, $NH(^1\Delta)$ is consumed by reactions (3) and (7), while N_2O is formed by reaction (2). Denoting the rate constants for reactions (3) and (7) by k_3 and k_7 and noting that the effective rate constant for reaction (2) should be $k_2=\eta k_3$, we may write

$$\Phi(N_2O)=\frac{\eta(k_3/k_7)x_{NO}}{(k_3/k_7)x_{NO}+1-x_{NO}} \qquad (8)$$

as a more reasonable expression of $\Phi(N_2O)$ as the function x_{NO}. Eq. (8) reduces to $\Phi(N_2O)=\eta x_{NO}$, when $k_3/k_7=1$.

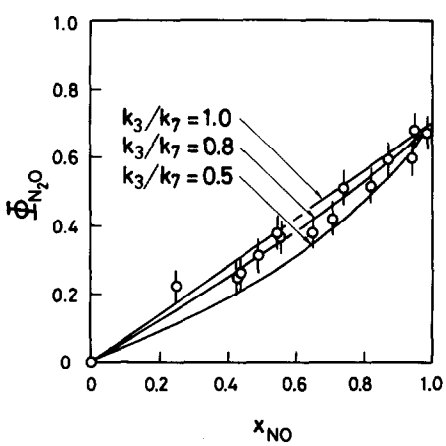

Fig. 4. Quantum yields $\Phi^*(N_2O)$ as the functions of the initial fractional concentration of NO. $x_{NO}=[NO]_0/([NO]_0+[HN_3]_0)$

Variations in $\Phi(N_2O)$ as a function of x_{NO}, eq. (8), for the varying ratio k_3/k_7 are represented by the curves shown in fig. 4. The ratio k_3/k_7 giving the best fits of the experimental data points to eq. (8) has been searched for by the least-squares treatment of the data under the constraint $\eta=0.70$. The resulting k_3/k_7 ratio was found to be 0.79 ± 0.06, the uncertainty limit indicating the probable error. The rate ratio between reactions (2) and (7) will then be $k_2/k_7=0.55\pm0.05$. The result can be taken as an indication that, if reaction (2) is a collision-controlled (no-activation-barrier) process, so will reaction (7) be essentially. Reaction (7) should be about twice as fast as reaction (2).

Mass-spectrometric analyses of the product mixtures have indicated that, in the runs where x_{NO} is relatively small, a sizable amount of H_2O has been formed concurrently. Occurrence of H_2O must somehow be related to reaction (7). We assume that the formation of H_2O is ascribable to the reaction

$$NH_2+NO\rightarrow[H_2N\text{–}NO]\rightarrow H_2O+N_2\,, \qquad (9)$$

which will immediately follow reaction (7). Because H_2O has been formed concurrently with N_2O and because both reactions (2) and (7) are likely to be collision-controlled, reaction (9) must also be a collision-controlled process.

4. Discussion

As has already been mentioned, the accuracy limit of the present CI calculations is at best 20 kJ/mol for stable energy minima. The situation requires particular cautions on the reliability of the energies calculated here for the various transition states.

The transition states of utmost importance in this work are TS1 and TS2. Some assessments of the energetics calculated for these states are possible in reference to the experimental kinetic results [17] for the reaction

$$N_2O+H \rightarrow [HNNO] \rightarrow N_2+OH\,. \qquad (10)$$

The transition states for the first and second steps of reaction (10) are nothing but our TS1 and TS2, respectively. According to the results of our CI calculations, the barrier height for the first step is 78 kJ/mol while that for the second step relative to N_2O+H is 91 kJ/mol (see fig. 3). When the vibrational zero-point energy corrections are made, these barrier heights are slightly enhanced to $\Delta H^{\ddagger}=79$ and 96 kJ/mol, respectively. The experimental study of reaction (10) shows that the second step is rate-controlling and that the net activation energy relative to N_2O+H is 81 kJ/mol [17]. Our predicted heats of activation ($\Delta H^{\ddagger}$) are in harmony with the experimental results, although $\Delta H^{\ddagger}=96$ kJ/mol for the second step is still 15 kJ/mol too high as compared to the experimental activation energy (81 kJ/mol). We believe that the accuracy of the present calculations is within a range of 20 kJ/mol even for the transition states. Incidentally, the MP4 calculations with the bond-additivity corrections (BAC) and spin contamination corrections by Marshall et al. [17] give the heats of activation 15 and 70 kJ/mol for the steps 1 and 2, respectively. Their results are significantly lower than the $\Delta H^{\ddagger}$ values (79 and 96 kJ/mol) obtained in the present study.

The theoretical expectation that the reaction between $NH(^1\Delta)$ and NO gives N_2O as the ultimate principal product has been corroborated experimentally. The reaction should be a two-step process involving the intermediacy of the adduct radical HN–NO($^2A'$). Because the barrier top of the subsequent step, i.e. the N–H bond cleavage of the adduct radical (reaction (4b)), lies below the energy level for the initial binary system $NH(^1\Delta)+NO$, the initial association step (3) should control the overall rate of reaction. Thus, reaction (2) as a whole should essentially be a collision-controlled process, which has no activation energy.

Under our experimental conditions, $NH(^1\Delta)$ should react with HN_3 also (reaction (7)). The bimolecular rate constant 5.6×10^{13} cm^3 mol^{-1} s^{-1} observed for reaction (7) [22] indicates that the reaction is indeed collision controlled. Reaction (7) competes with reaction (2), thus affecting the quantum yield of N_2O. It is our feeling that reaction (7) is also a two-step process involving the initial insertion of $NH(^1\Delta)$ into the NH bond of HN_3.

The decrease in $\Phi(N_2O)$ with the decreasing initial molar ratio of NO (fig. 4) is counterbalanced by the increase in the yield of H_2O. We interpret this fact to be a consequence of the operation of reaction (9) which immediately follows reaction (7). So far as both HN_3 and NO are present in large excess over $NH(^1\Delta)$ as is actually the case, all the NH_2 radicals formed by reaction (7) will be led to H_2O if reaction (9) is assumed to be as rapid a process as the collision-controlled reaction (7). This last assumption seems to find support in the potential energy profiles calculated by Melius and Binkley [6]. The reaction is reported to be a multi-step process which involves the intitial association of NH_2 with NO to form H_2NNO and the subsequent H-atom migrations, thereby ending up with the formation of H_2O and N_2 as stable products. They conclude that the various barriers which the adduct molecule has to overcome before reaching the final state H_2O+N_2 all lie below the energy level for the initial state NH_2+NO. Reaction (9) can, therefore, be considered to proceed as rapidly as most association reactions which are basically collision controlled. In fact, the rate constants observed for reaction (9) in the ordinary temperature region is on the order of 1×10^{13} cm^3 mol^{-1} s^{-1} [23].

The quantum yield of N_2O in the high NO fractional limit $x_{NO}=1$ is 0.7. The remaining fraction 0.3 is probably ascribable to the operation of reaction (4c) as a less favorable fragmentation process of 4C. Although no special efforts have been made to determine the branching ratios of reaction (4) in this work, the partial rate factor as large as 0.3 for reaction (4c) is a likely possibility, since TS2 is calculated to be only slightly (by 13 kJ/mol) higher than TS1. Frag-

mentation to $NH(^3\Sigma^-)+NO$ will be much less favorable. Direct quenching of $NH(^1\Delta)$ to $NH(^3\Sigma^-)$ on collisions with NO will also be ignorable [1].

Finally, we would like to comment on the observed rate ratio $k_3/k_7=0.79$ briefly. Because reactions (3) and (7) are both collision controlled, the relative rate constants k_3 and k_7 will be governed by the relative magnitudes of their pre-exponential factors. If so, the trend that $k_3/k_7 \lesssim 1$ is reasonable in view of the inherently smaller collision diameter for NO as compared to NH_3 which is apparently a larger molecular species. In addition, the insertion of $NH(^1\Delta)$ into propane, a chemical reaction which is also a no-activation-barrier process, is reported to have the rate constant k_{1a} 0.30 times as large as k_7 [1]. The tendency that $k_{1a}/k_7 < k_3/k_7$ is also reasonable in view of the difference in type between reactions (1a) and (3); the former reaction is a concerted multi-site process, whereas the latter is essentially a simple association reaction, for which the activation entropy should be innately larger.

Acknowledgement

This work was supported in part by the Grant-in-Aid No. 61470007 from the Ministry of Education, Japan. The authors are grateful to Dr. O. Kajimoto for advices in experiments and to Professor R.J. Buenker for a supply of his TABLE MRD CI program. They are also indebted to the Computer Center, Institute for Molecular Science for an allocation of cpu time.

References

[1] O. Kajimoto and T. Fueno, Chem. Phys. Letters 80 (1981) 484;
O. Kondo, J. Miyata, O. Kajimoto and T. Fueno, Chem. Phys. Letters 88 (1982) 424.
[2] T. Fueno, O. Kajimoto and V. Bonačić-Koutecký, J. Am. Chem. Soc. 106 (1984) 406.
[3] T. Fueno, J. Mol. Struct. THEOCHEM, to be published.
[4] T. Fueno, V. Bonačić-Koutecký and J. Koutecký, J. Am. Chem. Soc. 105 (1983) 5547.
[5] M.K. Kasha and D.E. Brabham, Org. Chem. (NY) (1979) 1.
[6] C.F. Melius and J.S. Binkley, 20th Symposium (International) on Combustion (The Combustion Institute, Pittsburgh, 1984) p. 575.
[7] R. Ditchfield, W.J. Hehre and J.A. Pople, J. Chem. Phys. 54 (1971) 724.
[8] P.C. Hariharan and J.A. Pople, Theoret. Chim. Acta 28 (1973) 213.
[9] J.S. Binkley, R.A. Whiteside, R. Krishnan, R. Seeger, D.J. DeFrees, H.B. Schlegel, S. Topiol, L.R. Kahn and J.A. Pople, GAUSSIAN 80, QCPE No. 406.
[10] R.J. Buenker, in: Studies in physical and theoretical chemistry, Vol. 21, ed. R. Carbo (Elsevier, Amsterdam, 1982) p. 17.
[11] R.J. Buenker and R.A. Phillips, J. Mol. Struct. THEOCHEM 123 (1985) 291.
[12] S.R. Langhoff and E.R. Davidson, Intern. J. Quantum Chem. 8 (1974) 61.
[13] P.J. Bruna and S.D. Peyerimhoff, in: Ab initio methods in quantum chemistry, Part I, ed. K.P. Lawley (Wiley-Interscience, New York, 1987) p. 1.
[14] R.J. Buenker, Intern. J. Quantum Chem. 29 (1986) 435.
[15] R.S. Konar, S. Matsumoto and B. de B. Derwent, Trans. Faraday Soc. 67 (1971) 1698.
[16] C.G. Hatchard and C.A. Parker, Proc. Roy. Soc. A 235 (1956) 518.
[17] P. Marshall, A. Fontijn and C.F. Melius, J. Chem. Phys. 86 (1987) 5540.
[18] J. Alster and L.A. Burnell, J.Am. Chem. Soc. 89 (1967) 1261.
[19] J.M. Howell and L.A. Kirschenbaum, J. Am. Chem. Soc 86 (1967) 877.
[20] L.A. Curtiss, D.L. Drapcho and J.A. Pople, Chem. Phys. Letters 103 (1984) 437.
[21] S.W. Benson, Thermochemical kinetics, 2nd Ed. (Wiley, New York, 1976).
[22] R.J. Paur and E.J. Bair, J. Photochem. 1 (1972/73) 255; Intern. J. Chem. Kinetics 8 (1976) 139.
[23] L.J. Stief, W.D. Brobst, D.F. Nava, R.P. Borkowski and J.V. Michael, J. Chem. Soc. Faraday Trans. II 78 (1982) 1391.